

TTAN: Two-Stage Temporal Alignment Network for Few-shot Action Recognition

Shuyuan Li^{1,*}, Huabin Liu^{1,*}, Rui Qian¹, Yuxi Li¹, John See²

Mengjuan Fei³, Xiaoyuan Yu³, Weiyao Lin¹

¹Shanghai Jiao Tong University, Shanghai, China

²Heriot-Watt University Malaysia, Putrajaya, Malaysia

³Huawei Cloud, China

{shuyuanli, huabinliu, qruai9911, lyxok1}@sjtu.edu.cn, J.See@hw.ac.uk

{feimengjuan1, yuxiaoyuan}@huawei.com, wylin@sjtu.edu.cn

ABSTRACT

Few-shot action recognition aims to recognize novel action classes (query) using just a few samples (support). The majority of current approaches follow the metric learning paradigm, which learns to compare the similarity between videos. Recently, it has been observed that directly measuring this similarity is not ideal since different action instances may show distinctive temporal distribution, resulting in severe misalignment issues across query and support videos. In this paper, we arrest this problem from two distinct aspects – action duration misalignment and motion evolution misalignment. We address them sequentially through a Two-stage Temporal Alignment Network (TTAN). The first stage performs temporal transformation with the predicted affine warp parameters, while the second stage utilizes a cross-attention mechanism to coordinate the features of the support and query to a consistent evolution. Besides, we devise a novel multi-shot fusion strategy, which takes the misalignment among support samples into consideration. Ablation studies and visualizations demonstrate the role played by both stages in addressing the misalignment. Extensive experiments on benchmark datasets show the potential of the proposed method in achieving state-of-the-art performance for few-shot action recognition.

CCS CONCEPTS

• Computing methodologies → Computer vision.

KEYWORDS

few-shot, action recognition, temporal alignment

1 INTRODUCTION

Action recognition [4, 21, 27] has received considerable attention in the computer vision community due to the increasing demand for video analysis in real-world scenarios. In recent years, deep learning methods have dominated the field of video action recognition with convolutional neural networks (CNNs). Numerous labeled data empower these CNNs-based methods to train a discriminative classifier for novel classes. Nevertheless, in a real sense, the number of novel action categories may be limited. This problem is compounded by the laborious and expensive task of annotating all available videos for these novel categories. Consequently, the few-shot learning (FSL) task, which aims to recognize novel visual categories from

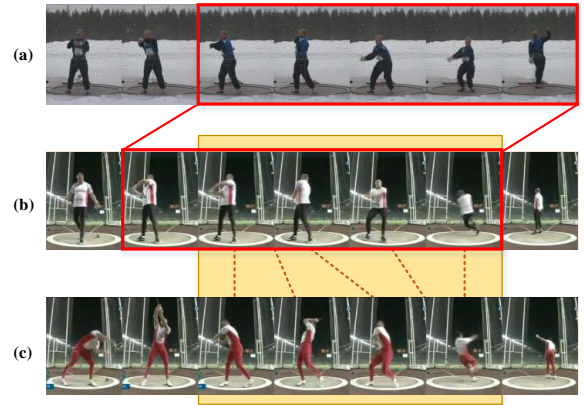


Figure 1: Example of misalignment. (a)&(b): action duration misalignment. The action duration is highlighted in red rectangle. (b)&(c): motion evolution misalignment. The dash lines means this pair of frames are consistent in motion evolution.

very few labeled examples, has come into prominence in recent years. The solutions for image-based few-shot learning fall into three general categories: metric learning [17, 19, 25], data augmentation [8, 29], and optimization-based methods [16, 26]. Each of them has made impressive progress in general image recognition. However, fewer studies have been carried out on few-shot video action recognition. The majority of existing approaches in this area follow the metric learning-based paradigm [1, 2, 31], which learns to compare the similarity between the videos from known classes and videos from novel classes. Recently, some research works [2, 3, 30] observed that it is challenging to directly measure the similarity between videos due to the fact that different action instances show distinctive temporal distributions, e.g., different temporal locations or evolution processes, along the timeline in videos, can result in severe misalignment issues between the query and support videos. Some methods attempted to address this by performing temporal alignment, e.g., TARN [2] proposed a segment-by-segment attention module to perform temporal alignment at feature level; ARN [30] designed attention mechanisms to locate the discriminative temporal blocks. In contrast to these works, OTAM [3] explicitly aligned video sequences with dynamic time warping algorithm. Aligning the semantic content in videos is still challenging since there are a

* Equally contributed.

wide variety of techniques. As such, the problem of video alignment in few-shot action recognition remains quite under-explored.

In this paper, we delve into this specific problem in few-shot action recognition from two distinct aspects – both indicative of distinct misalignment issues. First, the relative temporal location of an action is usually inconsistent between videos due to different start time and duration (as shown in Figure 1(a)&(b)); in this paper, we define the issue of location inconsistency as **action duration misalignment** (ADM). Second, since action often evolves in a non-linear manner, the timestamp of the most discriminative part within the action process can be quite different among observed action instances (as shown in Figure 1(b)&(c)), even though they share the same semantic category and temporal location. We define this internal variation among action instances as **motion evolution misalignment** (MEM).

To cope with these two types of misalignment, we devise a Two-stage Temporal Alignment Network (TTAN) for few-shot action recognition. The first stage predicts temporal warp parameters for input video and then performs a temporal transformation on the feature sequence, aligning it with the action duration period. In the second step, a Temporal Attentive Module (TAM) is adopted to coordinate the motion evolution of query action video using a cross-attention mechanism. Besides, we devise a novel multi-shot fusion strategy for the multi-shot setting to relieve the misalignment among the support samples. Using our proposed two-step strategy, we aim to ensure that actions are well aligned in temporal duration and motion evolution. The detailed pipeline of our proposed method is illustrated in Figure 4.

In summary, our main contributions are as follows:

- We delve specifically into the misalignment problem in few-shot action recognition, devising a novel two-stage temporal alignment method to address it.
- The proposed two modules perform temporal transformation and cross-attention on input video sequences, which respectively addresses the action duration and motion evolution misalignment sequentially.
- For the multi-shot FSL, we devise a novel multi-shot fusion strategy, which considers the misalignment among support samples, to produce an aligned prototype for each support category.
- Extensive experiments conducted on benchmark datasets show that our proposed method is capable of achieving state-of-the-art results in few-shot video action recognition.

2 RELATED WORK

Few-shot Learning The challenge faced in FSL is the insufficiency of data in novel classes. The direct approach to address this is to enlarge the data scale by data augmentation. [8, 29] are proposed to generate unseen data with labels to enrich the feature spaces of novel classes. Autoaugment further automatically learns the augmentation policy to improve the generalization on various few-shot datasets. Learning metrics to compare the known and novel classes is another branch of FSL. Matching network [25] is an end-to-end trainable kNN model using cosine as the metric, with an attention mechanism over a learned embedding of the labeled samples to predict the categories of the unlabeled data. Prototypical

Network [17] uses a feed-forward neural network to embed the task examples and perform nearest neighbor classification with the class centroids. [19] proposes a novel network which concatenates the feature maps of two images, sending the concatenation to a relation net to learn the similarity. While these methods perform well on image recognition tasks, it is not appropriate to transfer them directly to action recognition.

Action Recognition The state-of-the-art action recognition methods focus on designing architectures for temporal modeling in videos. C3D [21] and I3D [4] are the most representative networks that extend VGGNet and InceptionNet to 3D convolution version for extracting temporal information of videos, respectively. However, this simple extension leads to expensive computational costs and memory demand. Therefore, recent researches pay more attention to efficient action recognition models. P3D [15] and R(2+1)D [22] decompose the 3D convolution into a 2D convolution and a 1D convolution to learn the spatial and temporal information separately, which gains a lower computational costs and higher accuracy. Besides, some approaches were proposed to better capture temporal relation. Non-Local [28] is a generic operation similar to self-attention, which is able to capture the long-term spatio-temporal dependence. Based on TSN [27], TRN [2] was proposed to learn and reason about temporal dependencies between video frames. Different from the above, SlowFast [6] involves a network with dual paths to capture the spatiotemporal features; convolutions operate at low and high video frame rates to capture spatial semantics and motion information.

Few-shot Action Recognition The early study on few-shot action recognition could be traced to CMN [31], which proposed a compound memory network to store matrix representation. It can be easily retrieved and updated in an efficient way. The majority of current studies on few-shot action recognition follow the metric learning paradigm. TAEN [1] encodes actions in videos as trajectories in a metric space by a collection of temporally ordered sub-actions, then a FAN [20] condenses the motion feature of video into a single dynamic image, which relieves the pressure of learning the distance metrics. Due to the various temporal location of actions in videos, directly comparing the similarity of two videos with misaligned actions may lead to a trivial distance metric. To solve this issue, some approaches are proposed to perform the temporal alignment. TARN [2] proposed an attentive relation network to perform the temporal alignment implicitly at the video segment level. OTAM [3] explicitly aligns video sequences with a variant of the Dynamic Time Warping (DTW) algorithm. ARN [30] generates attention masks to re-weight the spatiotemporal features. Moreover, the augmentation strategy with self-supervised learning is also utilized to enhance the feature encoder and attention mechanism. Recently, TRX [14] represents video by exhaustive pairs and triplets of frames, which allows comparison between all possible sub-sequences. Moreover, it employs temporal CrossTransformer to search the closest matching combination of query samples among support samples. However, such exhaustive representation and attention brings high computational complexity of $O(KT^6)$. Among these methods, OTAM and TRX are the most related work to ours.

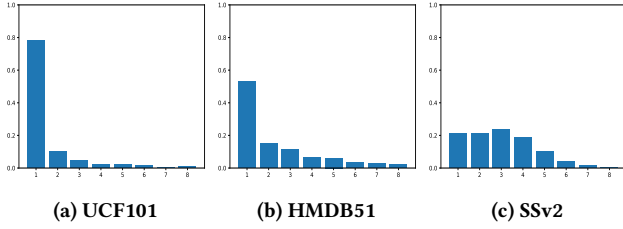


Figure 2: The action start time distribution on three datasets.

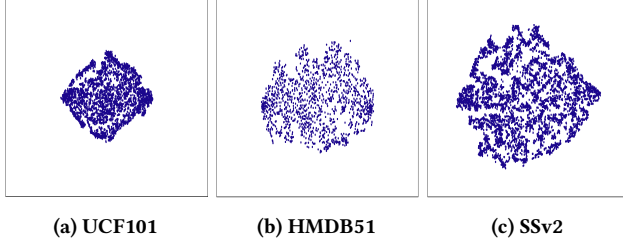


Figure 3: t-SNE plots for the probability sequences on three datasets.

3 DEALING WITH TEMPORAL MISALIGNMENT

To further analyze the temporal misalignment for actions, we quantify and compare these two types of misalignment on the three video action datasets (UCF101 [18], HMDB51 [12], SSv2 [7]). Firstly, we train a general action recognition model TSM [13] on each dataset separately. Given the well-trained classifier, we fed videos with T uniformly sampled frames into it and obtain the frame-level class probability vector $\mathcal{P} \in \mathbb{R}^{C \times T}$, where C denotes the number of classes. For each video, we extract the class-specific probability sequence $P = [p_1, \dots, p_T] \in \mathbb{R}^T$ from \mathcal{P} according to its ground-truth category. This class-specific probability vector is able to represent the evolution of action within T frames.

For the *action duration misalignment (ADM)*, we aim to analyze the distribution of action start time in different datasets. For each video, we consider the frame index t that satisfies $p_t \geq 0.5$ and $p_{1, \dots, t-1} < 0.5$ as the *start time*. The start time distributions for the three datasets are presented in Figure 2. For UCF101 and HMDB, the start time is distributed mainly over the first or second frame due to the fact that most videos are trimmed. On the contrary, the start time on the SSv2 dataset is evenly distributed over the first four frames. This demonstrates that the actions on the SSv2 dataset are more likely to execute at various time periods, which leads to more misalignment on action start and duration time.

For the *motion evolution misalignment (MEM)*, based on the probability sequence, we calculate the cosine similarity for all video pairs in each dataset. Then, we can quantify MEM for each dataset by the following operation:

$$MEM = \frac{1}{M} \sum_{i,j} [1 - \cos(P_i, P_j)], \text{ for all } (i, j) \text{ pairs} \quad (1)$$

where $M = 2 \cdot v_{num} \cdot (v_{num} - 1)$ is the normalization coefficient, v_{num} is the number of videos in dataset, $\cos(\cdot)$ calculates the cosine

Table 1: The estimated motion evolution misalignment (MEM) score on three datasets

Dataset	UCF101	HMDB51	SSv2
Estimated MEM	0.1653	0.3697	0.6260

similarity for pair of input. The estimated MEM scores for the three datasets are listed in Table 1. It can be seen that all datasets suffer from the MEM problem. Similar to the ADM, the problem of MEM is the most serious on the SSv2. Among these datasets, the UCF101 has a lower severity of evolution misalignment. Because it mainly consists of sports videos, which are more consistent in evolution for the same sports category. Furthermore, we also visualize the all probability sequences on a 2-dimensional coordinate figure using the t-SNE [23] in Figure 3. We can observe that it appears a concentrated distribution on UCF101 and HMDB51 while the distribution is more discrete on the SSv2 dataset. This also reveals that the SSv2 faces a more serious MEM problem. Overall, from the analysis above, we can conclude that the temporal misalignment problem widely exists in these three datasets. The problem reaches the most serious level on the SSv2 dataset. Meanwhile, HMDB owns a great severity of misalignment than the UCF101 dataset, indicating that solving the temporal misalignment problem is critical for few-shot action recognition, especially on the SSv2 dataset. Based on the above observation, we introduce our proposed method that aims at addressing the misalignment problem.

4 METHODS

Figure 4 shows the outline of our methods. In the following, we first provide a formal problem set-up of few-shot action recognition, then introduce modules of our methods sequentially: the feature embedding module, TTM module, TAM module, and multi-shot fusion strategy. At last, we describe how to optimize our model.

4.1 Problem Set-up

Following the standard few-shot action recognition setting, the dataset is divided into three distinctive parts: training set C_{train} , validation set C_{val} , and test set C_{test} . The training set owns sufficient labeled data of each class while there exist only a few labeled samples in the test set. The validation set is only used to evaluate the model during training. Moreover, there is no overlapping category among these three sets. The few-shot action recognition aims to train a classification network that can well generalize to novel classes in the test set. In the specific N -way K -shot few-shot learning setting, each episode contains a support set \mathcal{S} sampled from the training set C_{train} . It contains $N \times K$ samples from N different classes where each class contains K support samples. Then Q samples from each class are selected to form the query set \mathcal{Q} which contains $N \times Q$ samples. The goal is to classify the $N \times Q$ query samples only with the $N \times K$ support samples.

4.2 Model

Feature Embedding Module. The feature embedding module is used to represent a video by dense frame-level features. Since there usually exist hundreds of frames and great redundancy in a

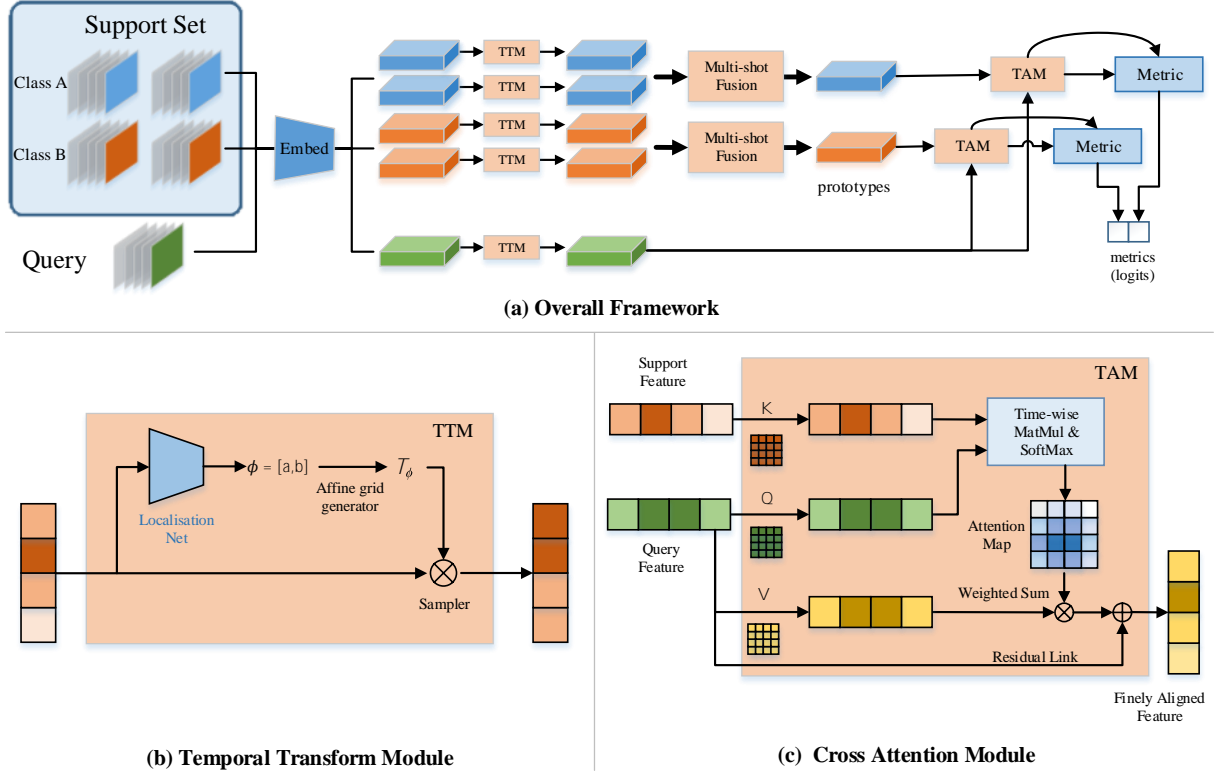


Figure 4: Framework of our methods. The 2-way 2-shot task is shown as example here.

trimmed video, frame sampling is generally adopted to select some representative frames from the whole video in order to reduce the computational complexity and redundancy. We follow the sampling strategy described in TSN [27], which divides a video into T segments and then samples uniformly in each segment. Thus, each video is represented by a fixed-length frame sequence. Given the frame sequence $X = \{x_1, x_2, \dots, x_T\}$, a feature embedding network $f(\cdot)$ takes it as input and embeds the sequence x into T frame-level features $\hat{f}_X = f(X) = \{f(x_1), f(x_2), \dots, f(x_T)\} \in \mathbb{R}^{C \times T \times H \times W}$. In the following, we use \hat{f}_s, \hat{f}_q to represent the video-level feature of the support sample and query sample, respectively.

Temporal Transform Module. In various vision tasks (e.g., image classification, pose estimation), the STN (Spatial transformer Network) [11] was introduced to allow for in-variances to spatial warps. Inspired by its idea, we design a Temporal Transform Module (TTM) to tackle the action duration misalignment. The TTM consists of two parts: a localization network L and an affine transformation T . Given an input frame-level feature sequence \hat{f}_X , the localization network generates warping parameters $\phi = (a, b) = L(\hat{f}_X)$, then the input feature sequence is warped by corresponding affine transformation T_ϕ parametrized by ϕ . The above temporal transform process can be formulated as:

$$\hat{f}_X' = T(\hat{f}_X, \phi = L(\hat{f}_X)) \quad (2)$$

where \hat{f}_X' indicates the feature sequence aligned to the action duration period, the L consists of several trainable layers in our implementation. Since the action duration misalignment appears linearly among videos, the warping is carried out using linear temporal interpolation. This also makes our entire pipeline differentiable and thus we can train our classifier with TTM jointly in an end-to-end manner. The framework of TTM is illustrated in Figure 4(b). During the episode training and testing, all the feature sequences of support and query samples are fed into the TTM to perform the first-stage temporal alignment, making the features roughly aligned to the duration of action. In this way, the action duration misalignment could be relieved by the first TTM stage.

Temporal Attentive module. The second type of misalignment, motion evolution misalignment, results from that actions evolve non-linearly in videos, which cannot be well addressed by the linear transformation-based TTM. To this end, we propose a Temporal Attentive Module (TAM) to align video features to consistent motion evolution for a better comparison. The TAM is based on a cross-attention mechanism, since key-query-value style attention mechanism [24] has been widely applied to many visual tasks [10, 28] and shows a solid ability to model relationships among instances.

Specifically, our TAM models the motion relation between video sequences in temporal dimension and then coordinates their action evolution features according to the relation. Given a pair of video features aligned by TTM: support feature \hat{f}_s and query features \hat{f}_q , the relation between their motion evolution is modeled by:

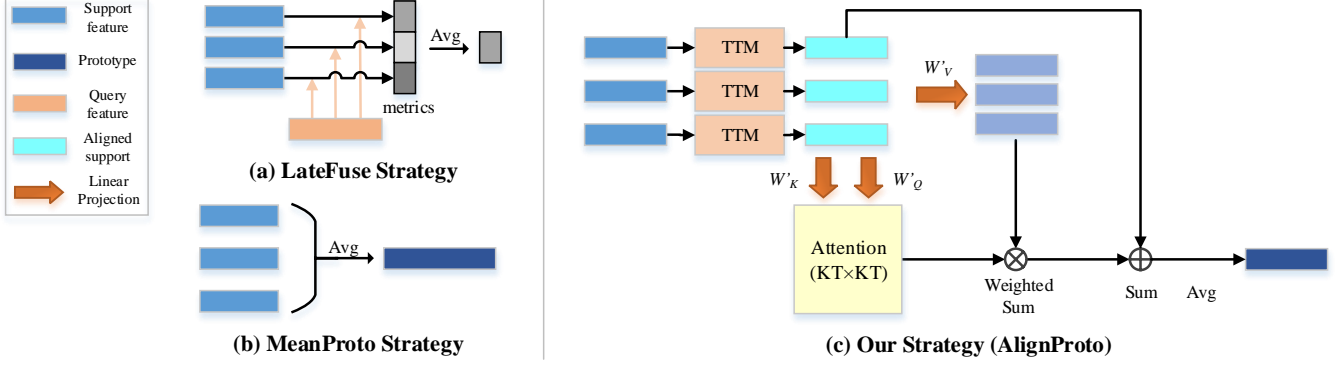


Figure 5: Illustration of different multi-shot fusion strategies.

$$M = \text{softmax}\left(\frac{(W'_k \cdot G(\hat{f}_s))(W'_q \cdot G(\hat{f}_q))^T}{\sqrt{\dim}}\right) \quad (3)$$

where W'_k, W'_q indicate the weight of key, query head in attention mechanism, \dim is the dimension of feature $G(\hat{f})$, $M \in \mathbb{R}^{T \times T}$ denotes the attention matrix between support and query. G is the global average pooling in spatial dimensions whose output shape is $C \times T \times 1 \times 1$, which means that the attention mechanism is only performed in the temporal dimension. According to the attention matrix M , we could coordinate the video feature sequence of query with the feature aligned to support sample:

$$\tilde{f}_q = \hat{f}_q + M \cdot (W'_v \cdot G(\hat{f}_q)) \quad (4)$$

$$\tilde{f}_s = \hat{f}_s + W'_v \cdot G(\hat{f}_s) \quad (5)$$

where W'_v is the weight of value head, \tilde{f}_q denotes the feature aligned by TTM and TAM. Note that in order to keep feature-space consistency, value head projection and residual sum are also applied to support feature \hat{f}_s . In this way, the motion evolution misalignment can be rectified by our proposed temporal attentive module.

In our framework, the video feature sequences of query and support samples undergo through TTM and TAM alignment modules. They perform duration alignment and evolution alignment sequentially, which advocates a better comparison and metric learning between the support and query sample. The overall of our framework is illustrated in Figure 4.

Multi-shot Fusion Strategy. In the k -shot ($k > 1$) FSL setting, there exist two traditional strategies to compare the query sample with multi-shot support samples under the metric learning paradigm: (1)*Latefuse*: Compare the query sample with k support samples by a specific distance metric, respectively. The final results are the average of k distance metrics (as shown in Figure 5(a)). (2)*MeanProto* [17]: produce a **prototype** by averaging the k -shot support features to represent the category. Then the query sample is directly compared to the single prototype (as shown in Figure 5(b)). However, these simple operations ignore the fact that temporal misalignment exists not only between support and query samples but also among support samples under the multi-shot setting.

To solve this issue, we devise a novel multi-shot fusion strategy termed *AlignProto*, which aims to fuse the aligned multi-shot support features to generate a more representative prototype. Specifically, the K support features are first fed into TTM to get the duration aligned video features $\hat{f}_s^1, \dots, \hat{f}_s^k$. Then, similar to TAM, we build the relation in temporal dimension over the support samples in multi-shot:

$$\hat{F}_s = \text{Concat}[\hat{f}_s^1, \dots, \hat{f}_s^k] \in C \times KT \times H \times W \quad (6)$$

$$M_s = \text{softmax}\left(\frac{(W'_k \cdot G(\hat{F}_s))(W'_q \cdot G(\hat{F}_s))^T}{\sqrt{\dim}}\right) \quad (7)$$

W'_k, W'_q and G play similar roles as W_k, W_q, G in Equation 4.2, $M_s \in \mathbb{R}^{KT \times KT}$ denotes the attention matrix among support samples. According to the attention matrix M_s , we can perform the in-support operation to update all the support features:

$$\tilde{F}_s = [\tilde{f}_s^1, \dots, \tilde{f}_s^k] = \hat{F}_s + M_s \cdot (W'_v \cdot G(\hat{F}_s)) \quad (8)$$

Finally, we can produce the aligned prototype for multi-shot support by calculating the mean of all aligned support features:

$$\text{AlignProto} := \tilde{p}_s = \frac{1}{k} \sum_{i=1}^k \tilde{f}_s^i \quad (9)$$

By reducing the misalignment between support samples in multi-shot, our devised *AlignProto* empowers our network to learn a more representative and discriminative prototype for each classes. The pipeline of it is illustrated in Figure 5(c).

Optimization. We train our model under the framework of ProtoNet [17] with standard softmax cross-entropy. Given the aligned feature of query sample \tilde{f}_q and the aligned support prototype for class c , we can obtain the classification probability as:

$$P(x_q \in c_i) = \frac{\exp(-d(\tilde{f}_q, \tilde{p}_s^{c_i}))}{\sum_{c_j \in C} \exp(-d(\tilde{f}_q, \tilde{p}_s^{c_j}))} \quad (10)$$

Then the classification loss is calculated as:

$$\mathcal{L}_{cls} = - \sum_{q \in Q} \mathbb{I}(q \in c_i) \log P(x_q \in c_i), \quad (11)$$

where \mathbb{I} is indicator function, and d denotes the distance metric and we adopt the time-wise cosine distance in our implementation. Q

Method	Publication	UCF101		HMDB51		SSv2	
		1-shot	5-shot	1-shot	5-shot	1-shot	5-shot
ARN [30]	ECCV2020	66.3	83.1	45.5	60.6	-	-
ProtoNet(TSN-res50) [17]	-	74.0	88.5	54.2	66.0	33.6	43.0
CMN-J [32]	PAMI2020	-	-	-	-	34.4	43.8
OTAM [3]	CVPR2020	79.9*	88.9*	54.5*	66.1*	42.8	52.3
TRX($\Omega=\{1\}$) [14]	CVPR2021	79.0*	95.9*	52.1*	76.1*	38.8	60.6
TRX($\Omega=\{2,3\}$) [14]	CVPR2021	78.2*	96.1	53.1*	75.6	42.0	64.6
TTAN(Ours)	-	80.9	93.2	57.1	74.0	46.3	60.4

Table 2: Few-shot action recognition results. The note * means our implement for OTAM and results trained from authors' code for TRX.

and C represent query set and corresponding collection of class label, respectively.

5 EXPERIMENTS

5.1 Datasets and baselines

Datasets We conduct experiments on three popular datasets:

UCF101 [18] contains 101 action categories and 13,320 videos. We follow the same protocol introduced in ARN [30], where 70/10/21 classes and 9154/1421/2745 videos are included for train/val/test respectively.

HMDB51 [12] contains 6,849 videos divided into 51 action categories. Each category contains at least 101 videos. We also follow the protocol of ARN [30], which takes 31/10/10 action classes with 4280/1194/1292 videos for train/val/test.

SSv2 [7] contains 220,847 videos with 174 action categories. We adopt the same protocol as OTAM [3] where 64/12/24 classes and 77500/1925/2854 videos are included for train/val/test.

Competitors We compare our method with recent FSL action recognition works related to temporal handling with state-of-the-art results, including CMN-J [32], ARN [30], OTAM [3], and TRX [14].

5.2 Implementation Details

We train and evaluate our model in a standard episode meta-learning way. In an N-way K-shot task setting, we sample $N \times K$ videos from N classes where each class has K samples as the *support set*. Additional $N \times Q$ examples are sampled from selected N classes as the *query set*. Support set and query set have no overlap. To be specific, 5-way 1-shot and 5-way 5-shot classification tasks are conducted on all datasets. For all datasets, we sample 8 frames uniformly for each video in the way introduced by TSN [27]. Extracted frames are first resized to 256×256 then random horizontal flip is applied. Then random crop (or center crop) with size (224,224) is applied during training (or testing). The input size for both training and testing is $3 \times 8 \times 224 \times 224$. Here 3, 8, and 224×224 are the channel dimension, the number of frames for each input clip, and the spatial resolution of each frame, respectively. We use the ImageNet pre-trained ResNet-50 [9] as the feature extractor so that we could have a fair comparison with previous methods [3, 14]. Specifically, the feature before the last *avgpooling* layer in ResNet-50 forms the frame-level input to our TTAN. During meta-training, we sample 200 episodes in single epoch. We train our model by SGD optimizer, with initial learning rate of 1×10^{-3} and momentum of 0.9. For UCF101 and HMDB51, the learning rate decays by 0.5 every 5 epochs. For SSv2,

the learning rate decays to 0.8 times every 30 epochs. We train our model for 100 epochs for UCF101 and HMDB51 and 400 epochs for SSv2. In testing, we sample 5000 episodes in the meta-test split and report the average result.

5.3 Main results

5.3.1 Quantitative Results. The quantitative results are listed in Table 2. As shown in this table, our method outperforms the powerful baseline ProtoNet on all datasets and is competitive with state-of-the-art methods. OTAM is the current SOTA method that focuses on temporal alignment, which is also the most related to ours. Compared with it, TTAN surpasses it by a significant margin on all settings and datasets. This demonstrates that our two-stage temporal alignment could better cope with the misalignment issue in few-shot action learning. TRX is the most recent approach which adopts the CrossTransformer [5] to build temporal relationships between videos. It allows the comparison between all sub-sequences and reaches a great performance on all datasets. However, it requires a great computational complexity for searching and comparing all possible frame pairs or triplets ($\Omega = \{2, 3\}$). Since input video sequences have been well-aligned in our method, we just need to compare the corresponding frame pairs rather than all combinations in TRX. Meanwhile, although we apply temporal cross-attention between query feature and support prototype, the prototypes can be computed offline. Thus, the overall complexity of our TTAN is $\frac{1}{K}$ and $\frac{1}{KT^4}$ of the TRX under $\Omega=\{1\}$ and $\Omega=\{2,3\}$ settings respectively, where K is the number of shot and T indicates the number of input frames. Nevertheless, our TTAN is still greatly superior to TRX under the 1-shot setting with such complexity reduction.

5.3.2 Qualitative Results and Visualizations. We visualize the temporal alignment results in stages to illustrate the effectiveness of our proposed method. The visualization results are presented in Figure 6, all presented videos are sampled from the test set. It can be observed that there exist duration and evolution misalignment between support videos and query video sequences. The alignment results of TTM are visualized by locating the action duration according to the predicted warp parameters. As shown in this figure, the duration of action is well-aligned by the TTM, which filters the insignificant background frame noise. Besides, the frame-wise similarity matrix is also calculated and presented for each pair of support features and query features (second row in Figure 6). We can observe that the features between videos are more consistent after undergoing through the TAM, which indicates that they are

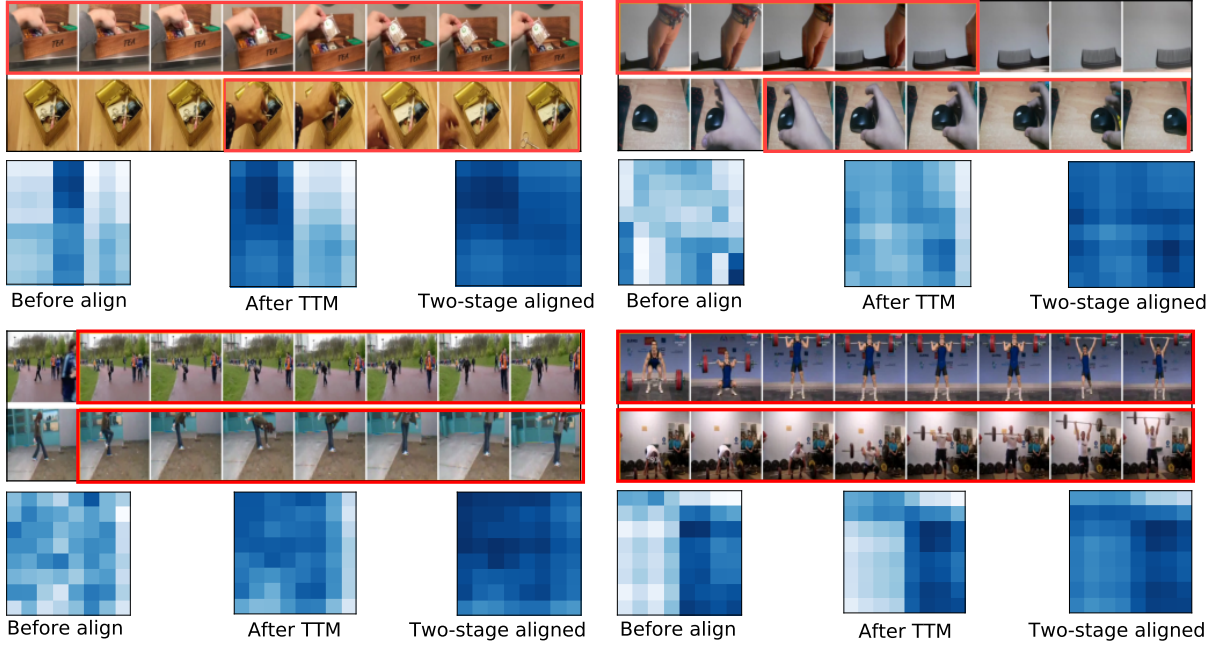


Figure 6: The visualization of temporal alignment result for each stage (examples from SSv2, SSv2, HMDB, UCF datasets, left to right and up to down). In the first two frame sequences, we visualize the aligned results of TTM on input support and query frames and highlight the aligned action duration in red color. The similarity matrix between video feature sequences are visualized for each stage below the frames.

Setting		UCF101	HMDB51	SSv2
TTM	TAM	1-shot	1-shot	1-shot
		74.0	54.2	40.1
✓		78.5	54.4	43.8
	✓	78.7	56.3	44.8
✓	✓	80.9	57.1	46.3

Table 3: Ablation of different modules of our proposed method on three datasets. ✓ means module is equipped.

aligned to a consistent motion evolution. In summary, the visualization reveals the effectiveness of our proposed TTAN.

5.4 Ablation Study

In this section, we perform extensive ablation experiments to verify the effectiveness of each proposed module.

5.4.1 Breakdown Analysis. Firstly, we break down our proposed TTAN and compare the performance gain of the TTM and TAM modules when applied separately. Quantitative results on HMDB51, UCF101, and SSv2 datasets are listed in Table 3. We can observe that both TTM and TAM boost the performance of few-shot action recognition, indicating each stage plays an important role in temporal alignment. When TTM and TAM are applied in a two-stage manner, the performance is further boosted. This supports that our two-stage design is able to well perform temporal alignment from two aspects. Our TTAN gains the most significant improvement on the SSv2. This finding also accords with our quantitative

Strategy	SSv2
LateFuse	52.8
MeanProto	57.6
AlignProto (Ours)	60.4

Table 4: Ablation of different multi-shot fusion strategy on SSv2 under 5-way 5-shot setting. TAM module is used after multi-shot fusion.

analysis on misalignment, where SSv2 manifests the most serious misalignment problem. This further demonstrates the effectiveness of our alignment modules. Although the UCF101 owns a relatively slight misalignment problem, our TTAN could still improve its performance by learning a more consistent temporal feature.

Moreover, since the OTAM [3] focus on temporal alignment, we would like to compare our individual temporal module to it. By comparison, either our single TTM or TAM outperforms it by a slight margin on all datasets. Compared with OTAM, our proposed temporal alignment modules are free from the problem of non-differentiable and easier to implement and train. Moreover, our TTAN can align actions in the continuous temporal dimension while the OTAM only learns a discrete temporal alignment.

Taken together, all the above results support that our proposed TTAN provides an effective way to address these two critical misalignment problems in few-shot action recognition task.

5.4.2 Multi-shot Fusion Strategy. To verify the effectiveness of our proposed multi-shot fusion strategy, we test and compare

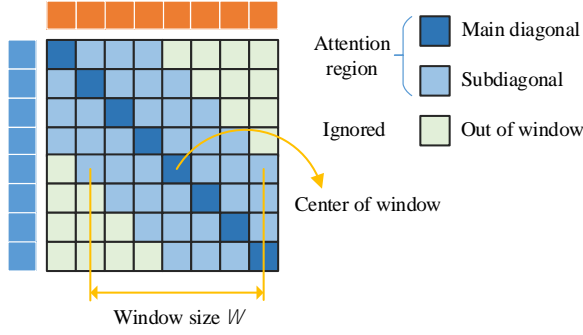


Figure 7: TAM with local attention. $W = 7$ for example.

Window size	3	5	7	Full
Accuracy	46.5	46.2	46.1	46.3
Attention Area	22	34	44	64

Table 5: Accuracy of TTAN and attention area w.r.t different window sizes of TAM, evaluated on SSv2 under 5-way 1-shot setting.

various strategies for shots fusion. Specifically, we perform 5-shot experiments on the SSv2 datasets and adopt different strategies (*Latefuse*, *MeanProto*, and *AlignProto*) separately, the comparison results are listed in Table 4.

Since the support-query video feature pairs have been well-aligned by our designed modules, we could see that the TTAN has reached a competitive performance with these two simple operations (*Mean* & *Latefuse*) on multi-shot. However, our proposed *AlignProto* strategy further improves its performance with a large margin, which achieves the state-of-the-art level. This indicates the temporal misalignment between different support samples is also critical for few-shot action recognition under multi-shot setting, which can be well handled by our fusion strategy.

5.4.3 Local Attention in TAM. In our TAM, the attention map $M \in \mathbb{R}^{T \times T}$ is performed over the $T \times T$ frames between query and support videos. However, since the action durations are well-aligned by TTM in the first stage, the global temporal attention may not be necessary. With this insight, we test the *local attention* TAM that performs cross-attention within only neighboring frames. The specific operation is illustrated in Figure 7, cross-attention is limited in a window. By reducing the window size of local attention, we can achieve the trade-off between accuracy and inference speed or computational complexity. With full attention window size (the original global TAM), our TAM can achieve the best performance with an acceptable computational complexity of $O(T^2)$ under all k -shot settings. By reducing the window size W , the complexity of the TAM module can be further reduced to $O(TW - \frac{W^2}{4})$ at the expense of accuracy, where T denotes the number of input frames. We evaluate the accuracy and corresponding attention area under different window sizes of TAM module as listed in Table 5.

Surprisingly, there only exists a slight performance decline following the reduction of attention window size. Moreover, the performance with $W = 3$ even outperforms the global attention TAM. This can be attributed to two reasons: (1) The TTM in our first stage has well-aligned the action duration for pair of videos. (2) Focusing

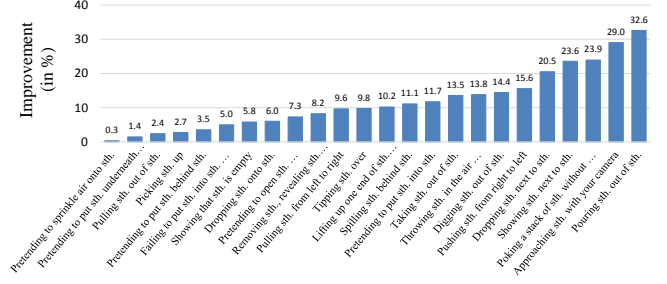


Figure 8: Class improvement using TTAN compared to the Prototype baseline for SSv2.

Representation	Method	Shot				
		1	2	3	4	5
Frame	OTAM [3]	42.8	-	-	-	52.3
	TRX{1} [14]	38.8	49.7	54.4	58.0	60.6
	TTAN(Ours)	46.3	52.5	57.3	59.3	60.5
Tuples	TRX{ $\Omega=2,3$ }	42.0	53.1	57.6	61.1	64.6

Table 6: Accuracy under 1- to 5-shot settings on SSv2. Note that our TTAN only uses single frame representation, equivalent to $\Omega = \{1\}$.

on the short-term temporal dependence is beneficial for our TAM, since the feature of frame pairs with large temporal distance shares less similar semantic information.

5.4.4 Class improvement. The improvement on the SSv2 dataset for each category using our TTAN is presented in Figure 8. What stands out in the figure is that the performance increases in all the categories. Moreover, some categories’ accuracy (e.g. “pouring sth out of sth”, “approaching sth”, “poking a stack of sth”) rise sharply ($> 20\%$ improvement). Interestingly, these action classes are also more vulnerable to the misalignment problem.

5.4.5 k-shot results. For completeness, we also provide the 2-, 3-, 4-shot results for TTAN in Table 6. Besides, the results of TRX are also listed for a comprehensive comparison. It’s apparent that a steady increase in the performance exists with more shots. What’s more, the comparison illustrates our TTAN surpasses the TRX under the same setting ($\Omega = 1$) for all k -shot. Surprisingly, compared with TRX ($\Omega = 2,3$) that uses pair and triplet frame representation, TTAN still outperforms it under 1~2 shot with a great margin. As for 3~5 shot setting, TTAN is also comparable with it.

6 CONCLUSION

This paper delves into the temporal misalignment issue in few-shot action recognition and proposes Two-stage Temporal Alignment Network (TTAN) to address it. It consists of two temporal alignment modules. The first performs temporal transformation to handle the action duration misalignment, while the second stage utilizes a cross-attention mechanism to coordinate the motion evolution misalignment. Meanwhile, a novel multi-shot fusion strategy is devised to address the misalignment among supports. Extensive experiments validate the effectiveness of the proposed TTAN.

REFERENCES

- [1] Rami Ben-Ari, Mor Shpigel, Ophir Azulai, Udi Barzelay, and Daniel Rotman. 2020. TAEN: Temporal Aware Embedding Network for Few-Shot Action Recognition. *arXiv preprint arXiv:2004.10141* (2020).
- [2] Mina Bishay, Georgios Zoumpourlis, and Ioannis Patras. 2019. Tarn: Temporal attentive relation network for few-shot and zero-shot action recognition. *arXiv preprint arXiv:1907.09021* (2019).
- [3] Kaidi Cao, Jingwei Ji, Zhangjie Cao, Chien-Yi Chang, and Juan Carlos Nieves. 2020. Few-shot video classification via temporal alignment. In *Proceedings of the IEEE/CVF Conference on Computer Vision and Pattern Recognition*. 10618–10627.
- [4] Joao Carreira and Andrew Zisserman. 2017. Quo vadis, action recognition? a new model and the kinetics dataset. In *proceedings of the IEEE Conference on Computer Vision and Pattern Recognition*. 6299–6308.
- [5] Carl Doersch, Ankush Gupta, and Andrew Zisserman. 2020. CrossTransformers: spatially-aware few-shot transfer. *arXiv preprint arXiv:2007.11498* (2020).
- [6] Christoph Feichtenhofer, Haoqi Fan, Jitendra Malik, and Kaiming He. 2019. Slow-fast networks for video recognition. In *Proceedings of the IEEE/CVF International Conference on Computer Vision*. 6202–6211.
- [7] Raghav Goyal, Samira Ebrahimi Kahou, Vincent Michalski, Joanna Materzynska, Susanne Westphal, Heuna Kim, Valentin Haenel, Ingo Fruend, Peter Yianilos, Moritz Mueller-Freitag, et al. 2017. The "something something" video database for learning and evaluating visual common sense. In *Proceedings of the IEEE International Conference on Computer Vision*. 5842–5850.
- [8] Bharath Hariharan and Ross Girshick. 2017. Low-shot visual recognition by shrinking and hallucinating features. In *Proceedings of the IEEE International Conference on Computer Vision*. 3018–3027.
- [9] Kaiming He, Xiangyu Zhang, Shaoqing Ren, and Jian Sun. 2016. Deep residual learning for image recognition. In *Proceedings of the IEEE conference on computer vision and pattern recognition*. 770–778.
- [10] Han Hu, Jiayuan Gu, Zheng Zhang, Jifeng Dai, and Yichen Wei. 2018. Relation networks for object detection. In *Proceedings of the IEEE Conference on Computer Vision and Pattern Recognition*. 3588–3597.
- [11] Max Jaderberg, Karen Simonyan, Andrew Zisserman, and Koray Kavukcuoglu. 2015. Spatial transformer networks. *arXiv preprint arXiv:1506.02025* (2015).
- [12] Hildegard Kuehne, Hueihan Jhuang, Estíbaliz Garrote, Tomaso Poggio, and Thomas Serre. 2011. HMDB: a large video database for human motion recognition. In *2011 International conference on computer vision*. IEEE, 2556–2563.
- [13] Ji Lin, Chuang Gan, and Song Han. 2019. Tsm: Temporal shift module for efficient video understanding. In *Proceedings of the IEEE/CVF International Conference on Computer Vision*. 7083–7093.
- [14] Toby Perrett, Alessandro Masullo, Tilo Burghardt, Majid Mirmehdi, and Dima Damen. 2021. Temporal-Relational CrossTransformers for Few-Shot Action Recognition. *arXiv preprint arXiv:2101.06184* (2021).
- [15] Zhaoan Qiu, Ting Yao, and Tao Mei. 2017. Learning spatio-temporal representation with pseudo-3d residual networks. In *proceedings of the IEEE International Conference on Computer Vision*. 5533–5541.
- [16] Sachin Ravi and Hugo Larochelle. 2016. Optimization as a model for few-shot learning. (2016).
- [17] Jake Snell, Kevin Swersky, and Richard S Zemel. 2017. Prototypical networks for few-shot learning. *arXiv preprint arXiv:1703.05175* (2017).
- [18] Khurram Soomro, Amir Roshan Zamir, and Mubarak Shah. 2012. UCF101: A dataset of 101 human actions classes from videos in the wild. *arXiv preprint arXiv:1212.0402* (2012).
- [19] Flood Sung, Yongxin Yang, Li Zhang, Tao Xiang, Philip HS Torr, and Timothy M Hospedales. 2018. Learning to compare: Relation network for few-shot learning. In *Proceedings of the IEEE conference on computer vision and pattern recognition*. 1199–1208.
- [20] Shaoqing Tan and Ruoyu Yang. 2019. Learning similarity: Feature-aligning network for few-shot action recognition. In *2019 International Joint Conference on Neural Networks (IJCNN)*. IEEE, 1–7.
- [21] Du Tran, Lubomir Bourdev, Rob Fergus, Lorenzo Torresani, and Manohar Paluri. 2015. Learning spatiotemporal features with 3d convolutional networks. In *Proceedings of the IEEE international conference on computer vision*. 4489–4497.
- [22] Du Tran, Heng Wang, Lorenzo Torresani, Jamie Ray, Yann LeCun, and Manohar Paluri. 2018. A closer look at spatiotemporal convolutions for action recognition. In *Proceedings of the IEEE conference on Computer Vision and Pattern Recognition*. 6450–6459.
- [23] Laurens Van der Maaten and Geoffrey Hinton. 2008. Visualizing data using t-SNE. *Journal of machine learning research* 9, 11 (2008).
- [24] Ashish Vaswani, Noam Shazeer, Niki Parmar, Jakob Uszkoreit, Llion Jones, Aidan N Gomez, Lukasz Kaiser, and Illia Polosukhin. 2017. Attention is all you need. *arXiv preprint arXiv:1706.03762* (2017).
- [25] Oriol Vinyals, Charles Blundell, Timothy Lillicrap, Koray Kavukcuoglu, and Daan Wierstra. 2016. Matching networks for one shot learning. *arXiv preprint arXiv:1606.04080* (2016).
- [26] Duo Wang, Yu Cheng, Mo Yu, Xiaoxiao Guo, and Tao Zhang. 2019. A hybrid approach with optimization-based and metric-based meta-learner for few-shot learning. *Neurocomputing* 349 (2019), 202–211.
- [27] Limin Wang, Yuanjun Xiong, Zhe Wang, Yu Qiao, Dahua Lin, Xiaoou Tang, and Luc Van Gool. 2016. Temporal segment networks: Towards good practices for deep action recognition. In *European conference on computer vision*. Springer, 20–36.
- [28] Xiaolong Wang, Ross Girshick, Abhinav Gupta, and Kaiming He. 2018. Non-local neural networks. In *Proceedings of the IEEE conference on computer vision and pattern recognition*. 7794–7803.
- [29] Yu-Xiong Wang, Ross Girshick, Martial Hebert, and Bharath Hariharan. 2018. Low-shot learning from imaginary data. In *Proceedings of the IEEE conference on computer vision and pattern recognition*. 7278–7286.
- [30] Hongguang Zhang, Li Zhang, Xiaojuan Qi, Hongdong Li, Philip HS Torr, and Piotr Koniusz. 2020. Few-shot action recognition with permutation-invariant attention. In *Proceedings of the European Conference on Computer Vision (ECCV)*. Springer.
- [31] Linchao Zhu and Yi Yang. 2018. Compound memory networks for few-shot video classification. In *Proceedings of the European Conference on Computer Vision (ECCV)*. 751–766.
- [32] Linchao Zhu and Yi Yang. 2020. Label independent memory for semi-supervised few-shot video classification. *IEEE Annals of the History of Computing* 01 (2020), 1–1.